Proceedings of the 16th International Conference on Soil Mechanics and Geotechnical Engineering

doi:10.3233/978-1-61499-656-9-1663

Distinct element analysis of soil-pipeline interaction in sand under upward movement at deep embedment condition

Analyse par éléments discrets de l'interaction sol sableux-oléoduc soumis à un déplacement vertical dans des conditions d'enfouissement profond

S. Yimsiri
Department of Civil Engineering, Burapha University, Thailand

ABSTRACT

The distinct element analysis of the soil-pipeline interactions in sand under upward movements at deep embedment conditions is undertaken. Available analytical solutions provide a wide range of predicted peak dimensionless forces and there is limited information regarding the transition of the peak dimensionless force from shallow to deep embedment conditions. Recently, finite element analysis of soil-pipeline interactions at deep embedment conditions has been performed. In the current study, distinct element analysis is employed to reinvestigate this problem because it is considered that the distinct element analysis may give more accurate results due to its discontinuous nature which more closely simulates sand behavior. The obtained results are compared with the previously published results and it is found that the results from distinct element and finite element are consistent except for the case of dense sand at deep embedment. The possibilities of the discrepancy are discussed.

RÉSUMÉ

Ce papier présente une analyse par éléments discrets des interactions sol sableux-oléoduc soumis à un déplacement vertical dans des conditions d'enfouissement profond. Il existe un grand nombre de solutions analytiques pour déterminer la force adimensionnelle limite, cependant il existe peu de solutions simultanément valables à faibles et grandes profondeurs. Récemment, une analyse par éléments finis en conditions d'enfouissement profond a été menée. Dans la présente publication, ce problème est revisité par le biais des éléments distincts dont la nature discontinue est considérée comme plus représentative du comportement mécanique des sables. Les résultats ainsi obtenus sont en accord avec les résultas publiés précédemment dans la littérature à l'exception du cas des sables denses et profond. Les causes possibles de cette divergence sont discutées dans ce papier.

1 INTRODUCTION

The standard formulations of the force-displacement characteristics for soil-pipeline interactions in sand under upward movement are given by ASCE in the "Guideline for the Seismic Design of Oil and Gas Pipeline System (1984)". According to this, the peak force per unit length F_{peak} applied to a pipeline is obtained by the following equation.

$$F_{peak} = \bar{\gamma} H_c N_{qc} D \quad (1)$$

where $\bar{\gamma}$ is the effective unit weight of soil, H_c is the depth to the center of the pipeline, and D is the external pipe diameter. N_{qc} is the peak dimensionless force and is a function of soil friction angle and embedment ratio H_c/D. These recommendations are derived from the experimental data by Trautmann and O'Rourke (1983) of a pipe with $H_c/D \leq 13$.

Available analytical solutions give a wide range of predicted peak dimensionless forces and there is limited information regarding the transition of the peak dimensionless force from shallow to deep embedment conditions. Yimsiri et al (2003) have recently presented a design chart for deep embedment conditions using finite element analysis. In this study, the Distinct Element Method (DEM) is employed to investigate the same problem again. Due to its discontinuous nature, it is considered that DEM should better simulate the soil movement close to the pipe at large pipe displacement and, hence, may yield more accurate results to the problem. In the past, the DEM has been used mainly for the study of micromechanical behavior of sand. This study provides an example of the use of the DEM for more practical problem. The DEM analysis is firstly calibrated against large-scale tank tests data reported by Trautmann and O'Rourke (1983) to determine the micromechnical input parameters that are not possible to be estimated from laboratory tests. By calibrating the model, the DEM analysis is extended to deeper embedment conditions. The DEM results are compared with the previous study of the same problem using Finite Element Method (FEM) (Yimsiri et al., 2003).

2 DISTINCT ELEMENT ANALYSIS

The pipe loading experiments were simulated using the distinct element method based on the approach by Cundall and Strack (1979). The distinct element code PFC^{3D} (Itasca, 1999) was employed. The code models soil particles as a collection of distinct and arbitrarily sized spherical particles. The particles are treated as rigid bodies and allowed to overlap one another at the contact points. The contacts between particles are characterized through the stiffness and slip condition. The constitutive behavior of the particles enables the simulation of macroscale plasticity. No bonding between particles is employed in this study to simulate uncemented sand.

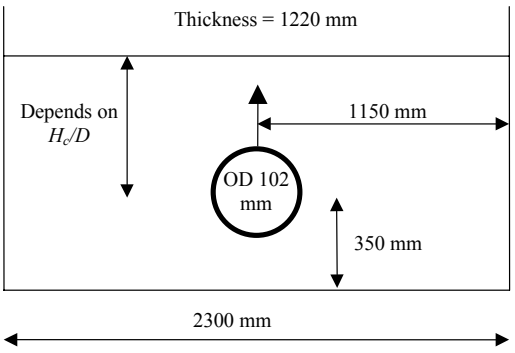

Figure 1. Schematic diagram of set-up of large-scale tank test.

DEM analysis requires knowledge of a force-displacement law at particle contacts. The linear elastic contact model was employed; the contact force and relative contact displacement are linearly related by a constant contact stiffness. Two stiffness values are required for each contact; they are (i) normal contact stiffness k_N and (ii) tangential contact stiffness k_T (force/displacement). Particle sliding occurs when the tangential contact force reaches its maximum allowable value, which is taken to be the coefficient of inter-particle friction angle between the two contacting entities multiplied by the magnitude of the normal contact force.

3 NUMERICAL MODELING

Trautmann and O'Rourke (1983) performed large-scale tank experiments at shallow depth to investigate the pipeline behavior. Their results were used here as benchmarks in order to examine the capability of the current DEM analysis technique. The schematic diagram of the test set-up is shown in Fig. 1. The tests were performed for different H_c/D values up to 13. Cornell filter sand was used for all the tests. It is a clean, subangular, fluvio-glacial sand, having a coefficient of uniformity C_u of 2.6 and an effective grain size D_{10} of 0.2 mm. The 102-mm pipe was fabricated from ASTM Grade A-36 steel. Soil-pipe interaction at three different densities was tested; 14.8 (loose), 16.4 (medium), and 17.7 (dense) kN/m^3, which corresponded to the relative density of 0, 45, and 80%, respectively. In practice, the sand placed around a pipeline is often in the state of medium to dense conditions. Hence, the behavior in medium and dense sands was of interest in this study and these test cases were simulated.

The tank and pipe were modeled by series of planar wall. The dimensions of the tank were the same as the actual tank. The tank wall was assumed to be smooth; the tank model has a normal contact stiffness equal to that of the particles but has zero tangential contact stiffness and zero surface friction. The pipe has identical contact stiffness in both normal and tangential directions and equal to that of the particles. The pipe has its surface friction angle equal to half of the inter-particle friction angle of sand (Yimsiri et al., 2003).

Sand is modeled as a collection of spherical particles and its size distribution follows normal distribution. The sand particles are modeled by using larger sizes than actual sand with varying sizes in various regions of the model (see Fig. 2). Due to computational limitation, it was not possible to model using the actual particle size (D_{10} = 0.2 mm and D_{60} = 0.52 mm). At the region near the pipe (Region A), the particles are smaller with $r_{average}$ = 12.5 mm and standard deviation = 2.5 mm (25 times larger than actual sand). Further away (Region B), the particles are larger with $r_{average}$ = 25.0 mm and standard deviation = 5.0 mm (50 times larger). For the cases with $H_c/D \geq 17$, there is Region C with the particle size of $r_{average}$ = 37.5 mm and standard deviation = 7.5 mm (75 times larger). This allowed the number of particles to be less than 130,000 for deepest case. An example of the DEM models is shown in Fig. 3.

4 DETERMINATION OF INPUT PARAMETERS

The input parameters for DEM modeling are listed in Table 1. Most of the parameters were determined by calibrating the numerical results with the experimental data of (i) triaxial test results of the sands used for the tank experiments (Turner and Kulhawy, 1987) and (ii) the actual pipe loading test results at shallow depths (Trautmann and O'Rourke, 1983).

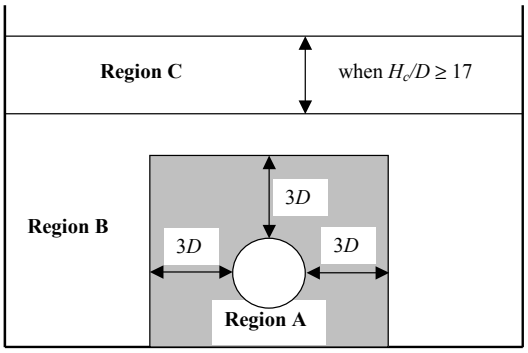

Figure 2. Various regions of the DEM model.

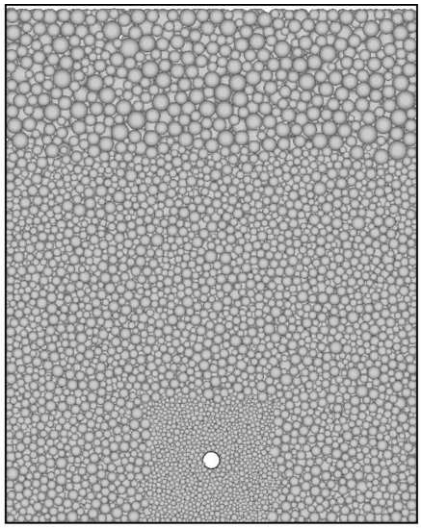

Figure 3. Example of DEM model (medium sand, H_c/D = 25).

Table 1: Input Parameters for DEM Analysis

Parameters	**Values**
Normal contact stiffness of particle, $k_{N,sand}$	From Eq. (2)
Tangent contact stiffness of particle, $k_{T,sand}$	$k_{T,sand} = k_{N,sand}$
Normal contact stiffness of pipe, $k_{N,pipe}$	$k_{N,pipe} = k_{N,sand}$
Tangent contact stiffness of pipe, $k_{T,pipe}$	$k_{T,pipe} = k_{N,pipe}$
Normal contact stiffness of wall, $k_{N,wall}$	$k_{N,wall} = k_{N,sand}$
Tangent contact stiffness of wall, $k_{T,wall}$	$k_{T,wall} = 0$
Inter-particle friction angle, $\phi_{\mu,sand}$	tan $\phi_{\mu,sand}$ = 0.5, 1.0, 3.0
Pipe friction angle, $\phi_{\mu,pipe}$	$\phi_{\mu,pipe} = \phi_{\mu,sand}/2$
Tank wall friction angle, $\phi_{\mu,wall}$	$\phi_{\mu,wall} = 0$
Density of particle, ρ (kg/m^3)	2740
Radius of particle, r	Varies in Regions A, B, C

Results from the triaxial test simulations show that the DEM analysis (using $k_N = k_T$) can simulate the stress-strain relationship by using a high value of inter-particle friction angle (tan ϕ_μ = 3.0) as shown in Fig. 4. This is due to the use of spherical particles, which allows excessive particle rolling (e.g. Thomas and Bray, 1999). The contact stiffness depends on confining

pressure (e.g. Yimsiri and Soga, 2000); however, it was not possible to derive the pressure-dependent stiffness values from the triaxial test results because the data did not span for a wide range of confining pressure. Instead, the contact stiffness was derived by fitting the DEM analysis results with the pipe loading data at shallow depths by using tan ϕ_μ = 0.5, 1.0, 3.0. The obtained relationship between the contact stiffness and the vertical effective stress at center of pipe is shown in Fig. 5 and the following relationships are proposed.

$$\left.\begin{aligned} k\,(\mathrm{N/m}) &= 6.714\sigma_c{}'^{3.813} \quad \text{for } \tan\phi_\mu = 0.5 \\ k\,(\mathrm{N/m}) &= 41.072\sigma_c{}'^{2.761} \quad \text{for } \tan\phi_\mu = 1.0 \\ k\,(\mathrm{N/m}) &= 112.859\sigma_c{}'^{2.176} \quad \text{for } \tan\phi_\mu = 3.0 \end{aligned}\right\} \qquad (2)$$

σ_c' (kPa) = vertical effective stress at center of pipe

It is noted that various combinations of the contact stiffness and tan ϕ_μ can yield similar peak forces. With larger tan ϕ_μ, the required contact stiffness is lower. It is interesting to find that the contact stiffness affects the strength (peak force) for this problem, which is not the case for triaxial problem where the contact stiffness affects only modulus, not strength. This may be due to the more complex mode of shearing in pipe loading problem. It is also noted that the obtained power is greater than 0.5 which is the normal value for soil (Hardin & Black, 1966); this may be also due to the complexity of mode of loading. The peak force values employed for fitting is governed by complex deformation at relatively large strain; however, the contact stiffness is the behavior at very small strain.

Examples of the computed force-displacement relationships are shown in Fig. 6. In case of medium sand, the results from all cases show small difference and match the experimental data well. However, for dense sand, the results from tan ϕ_μ = 0.5 show stiffest behavior which best match the experimental result, while other cases show more ductile behavior.

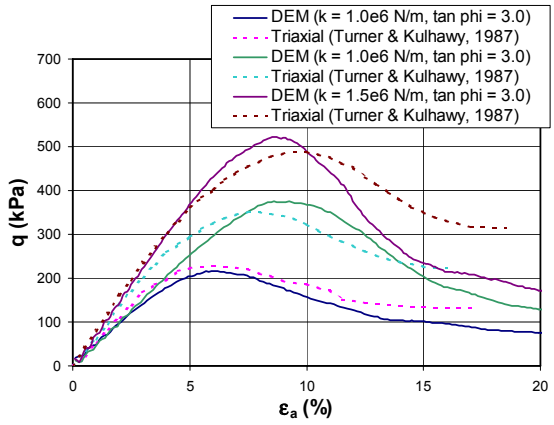

Figure 4. Calibration of DEM results against triaxial tests.

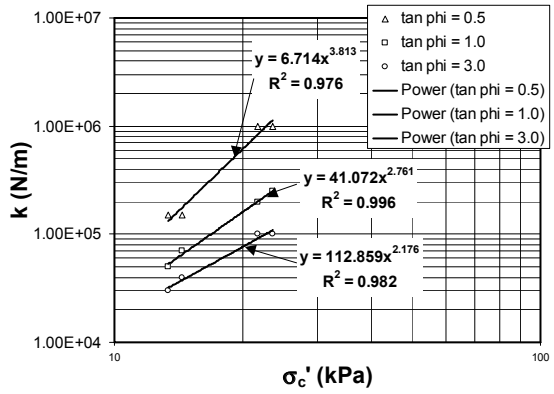

Figure 5. Relationship between contact stiffness and stress.

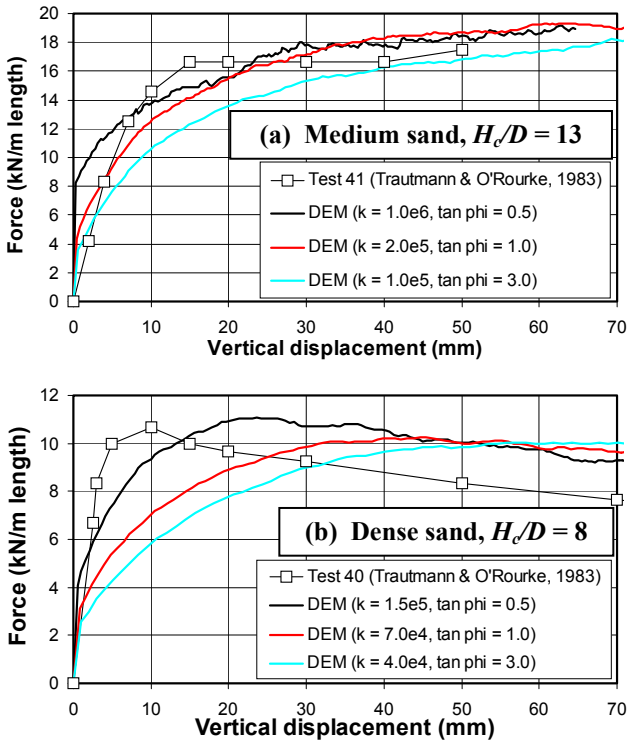

Figure 6. Calibration of DEM results against pipe loading tests.

5 RESULTS OF DEEP PIPE LOADING

After calibrating the DEM models with triaxial tests as well as the tank experiments, deep pipe loading cases were simulated using the input parameters derived from the shallow pipe loading cases. An example of the computed force-displacement curves are shown in Fig. 7 along with the result from the finite element analysis (Yimsiri et al., 2003). In case of medium sand, the results from DEM of all tan ϕ_μ cases are consistent with the FEM results. In case of dense sand, however, the result from DEM of tan ϕ_μ = 0.5 is considerably larger and the results become lesser for the cases of tan ϕ_μ = 1.0 and 3.0. The results for the case of tan ϕ_μ = 3.0 is closest to the FE result; however, its peak force is still somewhat larger. It is interesting to note that the DEM results of tan ϕ_μ = 0.5 better match the pipe loading test results at shallow depth, whereas the case of tan ϕ_μ = 3.0 better match the deep depth case.

Figure 8 shows the relationships between the peak dimensionless force and embedment ratio obtained from the DEM, FEM, and analytical solution by Meyerhof and Adams (1968). For some DEM simulations, the peak force was difficult to determine because the load-displacement curve exhibited ductile behavior with no distinctive peak. In such cases, the force-displacement data were fitted to a hyperbolic curve and the peak force was determined using the procedure used by Trautmann and O'Rourke (1983) for the actual test data. In case of medium sand, the DEM analysis of all tan ϕ_μ cases yield consistent results with FEM. In case of dense sand, however, the DEM analysis of all tan ϕ_μ cases yield consistent results with FEM only for $H_c/D \le 21$. When $H_c/D > 21$, the results from DEM become larger than FEM; the lesser the tan ϕ_μ employed (the larger the contact stiffness), the larger the overestimation. Only the case of tan ϕ_μ = 3.0 shows similar results to FEM with a tendency to give somewhat larger peak dimensionless force at deeper embedment depth ($H_c/D > 60$). The cases of tan ϕ_μ = 0.5 and 1.0 do not show any transition from shallow to deep failure. All results from numerical analysis (DEM and FEM) are larger

than the analytical solution by Meyerhof and Adams (1968) which is the only analytical solution that can predict the transition from shallow to deep failure.

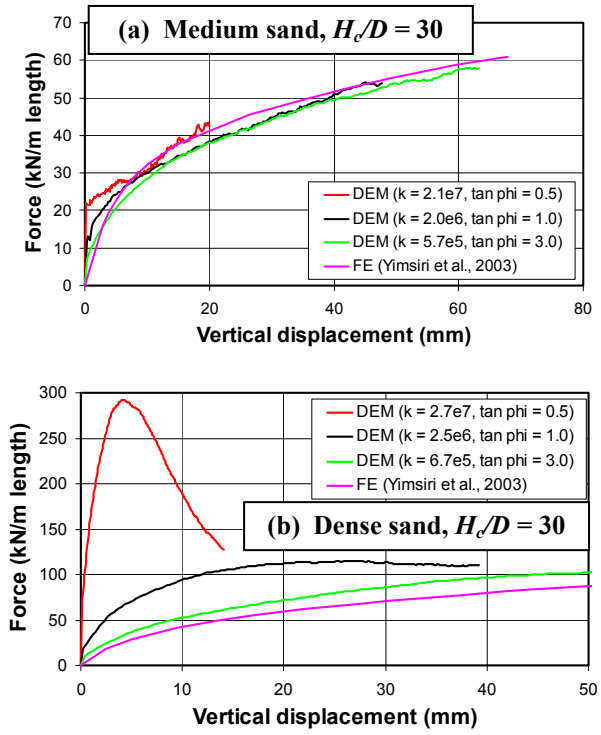

Figure 7. DEM results of deep pipe loading.

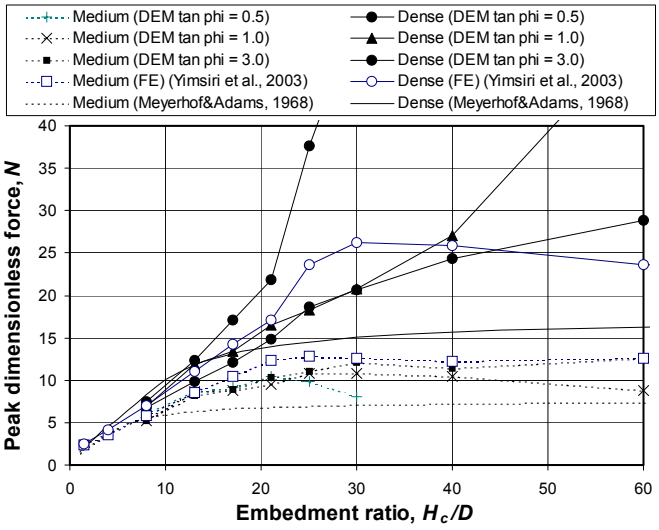

Figure 8. Comparison of peak dimensionless force.

6 DISSCUSSIONS

The displacement patterns from DEM and FEM for the case of shallow depth are quite similar. At deeper depth, the displacement pattern of medium sand shows local shear failure around pipe which is consistent with the deep shear failure behavior observed in Fig. 8. However, the displacement pattern of dense sand show overbreak failure, not local shear failure, and this tendency is more for lower tan ϕ_μ employed (higher contact stiffness) as can be seen from the steeper slope at deep depth in Fig. 8.

The advantage of DEM than FEM is its ability to present clearer movement of soil closely around the pipe due to the fact that the DEM analysis allows the soil particles to move freely. Also, the DEM analysis can continue with unlimited movement of the pipe until it reaches ultimate peak force (or further), unlike FEM which has to stop at some pipe displacement before peak force can be reached because large deformation of the mesh causes numerical convergence problem. The investigation of the particle movement around the pipe in detail is under way.

7 SUMMARY AND CONCLUSIONS

The soil-pipeline interactions under upward movements in sand were investigated using DEM analysis. The simulations were performed for both medium and dense sand conditions at different embedment ratios H_c/D from 8 to 60. The transition of the maximum dimensionless force from shallow to deep embedment conditions was observed and the critical embedment ratio and the corresponding critical maximum dimensionless forces were evaluated. The DEM results were also consistent with the previously published FEM results especially for the case of medium sand. For the case of dense sand, the DEM results show a tendency to give larger peak dimensionless force at deeper embedment depth ($H_c/D > 60$). This is due to the fact that the local failure was not achieved. The results from this DEM analysis together with earlier FEM analysis will serve as a Class-A predictions of the future full-scale tank test of this problem.

ACKNOWLEDGEMENTS

The Author would like to thank Dr. Kenichi Soga for his advice. This work is supported by a grant from the Thailand Research Fund (TRF).

REFERENCES

ASCE 1984. Guidelines for the Seismic Design of Oil and Gas Pipeline Systems

Cundall, P. A. and Strack, O. D. L. 1979. A discrete numerical model for granular assemblies. Geotechnique, 29(1), 47-65.

Hardin, B. O. and Black, W. L. 1966. Sand stiffness under various triaxial stresses. J. of Soil Mech. and Foundations, ASCE, 92(SM2), 27-42.

Itasca. 1999. PFC^{3D}, Version 2.0

Meyerhof, G. G. and Adams, J. I. 1968. The ultimate uplift capacity of foundations. Canadian Geotech J, 5(4), 225-244.

Thomas, P. A. and Bray, J. D. 1999. Capturing Nonspherical Shape of Granular Madia with Disk Clusters. J of Geotech and Geoenviron Eng, ASCE, 125(3), 169-178.

Trautmann, C. H. and O'Rourke, T. D. 1983. Behavior of Pipe in Dry Sand Under Lateral and Uplift Loading. Geotechnical Eng Report 83-7, Cornell University

Turner, J. P. and Kulhawy, F. H. 1987. Experimental Analysis of Drilled Shaft Foundations Subjected to Repeated Axial Loads Under Drained Conditions. Report to Electric Power Research Institute, Cornell University

Yimsiri, S. and Soga, K. 2000. Micromechanics-based stress-strain behaviour of soils at small strains. Geotechique, 50(5), 559-571.

Yimsiri, S., Soga, K., Yoshizaki, K., and Dasari, G. R. 2003. Soil-Pipelines Interaction in Sand under Upward Movement at Deep Embedment Condition. 12th Asian Regional Conference on Soil Mechanics and Geotechnical Engineering, 1, 891-894.